Rouse Model with Internal Friction: A Coarse Grained Framework for Single Biopolymer Dynamics

Bhavin S. Khatri*,† and Tom C. B. McLeish‡

Polymer and Complex Fluids Group, School of Physics and Astronomy, University of Leeds, Leeds LS2 9JT, U.K.

Received May 24, 2007; Revised Manuscript Received June 28, 2007

ABSTRACT: Recent work has highlighted an intimate link between the internal friction of single biopolymers and dynamics on an underlying energy landscape of conformational change. Here, we examine the coarse-grained dynamics of flexible biopolymers by incorporating local internal friction sources into the successful Rouse model of polymer dynamics. Our main result is a closed-form expression of the frequency response function of a Rouse chain with and without internal friction. We find that the regimes in which internal friction and solvent friction dominate are characterized by single-mode dumbbell ($|J(\omega \rightarrow \infty)| \sim \omega^{-1}$) and Rouse-like behavior ($|J(\omega \rightarrow \infty)| \sim \omega^{-1/2}$), respectively. A real-space analysis shows these behaviors are due to a frequency-dependent length of chain that can respond to perturbations. By distinguishing dissipation due to internal conformational change with that from the solvent, the RIF model provides a simple and generic basis for probing the structure and dynamics of single biomolecules in stretching experiments.

Introduction

The Rouse and Zimm models have provided a successful framework for the modeling of the dynamics of flexible polymers in melts and dilute solutions.[1−3] Their success lies in the generality of modeling a polymer as a one-dimensional linearly interconnected object with freely jointed links. It is well-known that such a coarse-grained description is equivalent to the behavior of more realistic models of polymer chains that include local backbone correlations and hopping dynamics, when examined at sufficiently large length scales.[3] Dissipation in the Rouse model arises through *external* friction as segments of the polymer move through the solvent or melt. As will be discussed, at low frequency and low stretch this is the dominant form of dissipation in polymers. However, recent studies of single biopolymer dynamics, using for example atomic force microscopy (AFM) experiments,[4−9] have indicated that at high stretch *internal* friction can be the dominant source of dissipation, as was shown for the polysaccharides dextran and cellulose.[10] The importance of measuring internal friction of biopolymers lies in its relationship to dynamics on an underlying energy landscape of conformational change, which in the case cellulose and dextran revealed an unexpected roughness to their biomolecular landscapes. Extracting this new source of *local* dynamical information from single-molecule stretching experiments requires coarse-grained polymer models that incorporate the effects of internal friction. In this paper, we study, within the Rouse framework, the coarse-grained properties of *flexible* polymers with local internal friction, as well as hydrodynamic friction with the solvent. We note a similar coarse-grained model was developed by Pourier and Marko,[11] relevant to the study of internal friction in *stiff* biopolymers, such as chromatin or DNA. Here, particular emphasis will be placed on calculating the linear response of the end-to-end vector of the polymer, since this is the most easily probed parameter in single-molecule stretching experiments.

Fundamentally, internal friction in flexible polymers arises due to microscopic barrier hopping processes,[10,12,13] just as solvent friction is related to barriers for solvent molecules to pass by each other.[14] An example, relevant to both synthetic and biological polymers is furnished by the dihedral angle rotations of the backbone of a polymer. These occur on an energy landscape that usually consist of three stable minima separated by barriers. Two analogous quantities can be related to the local static and dynamic flexibility of a polymer: a persistence length related to the spread or distribution of populations among dihedral states and a persistence time related to a hopping time over barriers between states.[12] From these microscopic considerations, these quantities in turn give rise to macroscopic notions of the local elasticity and internal friction of a polymer.[10] It is this latter quantity, the internal friction, treated as a phenomenological parameter, which is the focus of this paper and its influence on the coarse-grained properties of a flexible polymer.

There have been a number of studies of the effect of local internal friction in polymers as reviewed by Manke and Williams;[15] Kuhn and Kuhn[16] were the first to note that the chain end-to-end internal friction should vary inversely with the number of monomers N ($\sim\zeta_i/N$), unlike solvent friction whose total friction scales linearly with chain length ($N\zeta_s$). This arises since the dynamics of conformational change from internal barrier hopping is dependent on any one of N bonds flipping states, in contrast to the resistance from the solvent, which requires N simultaneous and concerted motions of the chain and solvent molecules in its vicinity. This contrasting behavior naturally give rise to Kuhn's theorem, as discussed by de Gennes,[12] which implies that for long chains dynamical resistance due to internal barriers will be negligible for the first long wavelength modes, when compared to solvent friction. More quantitative models were later developed, in understanding the high-frequency rheology of dilute polymer solutions, including both continuum [17−19] and matrix bead level[13,19] models of polymer dynamics. In the latter discrete bead approach, Bazua

* To whom correspondence should be addressed; E-mail: bhavin.khatri@physics.org.
† Current address: Soft Condensed Matter Group, Department of Physics, University of Surrey, Guildford, GU2 7XH, U.K.
‡ E-mail: t.c.b.mcleish@leeds.ac.uk.

10.1021/ma071175x CCC: $37.00
Published on Web 08/08/2007

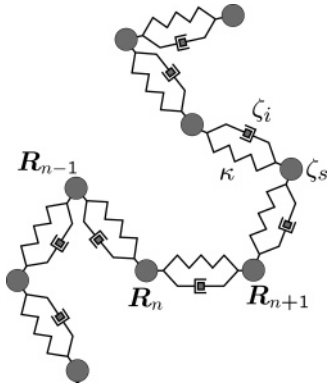

Figure 1. Schematic diagram of a RIF polymer, where beads with solvent friction ζ_s, are interconnected with springs and dashpots in parallel, of elastic constant κ and internal friction ζ_i, respectively.

and Williams showed by numerical computation, that in the limit where chains are long compared to their persistence length, local microscopic barrier hopping on a dihedral landscape gives rise to an internal friction force on the nth bead as $-\zeta_i(\dot{\boldsymbol{R}}_{n-1} - 2\dot{\boldsymbol{R}}_n + \dot{\boldsymbol{R}}_{n+1})$, where $\boldsymbol{R}_n$ is the position of the nth bead. In the continuum limit, this is equivalent to a force proportional to the rate of change of local curvature in the chain ($\partial_n{}^2\dot{\boldsymbol{R}}(n, t)$), as independently postulated by McInnes.[17]

The paper is organized as follows: first we develop the Rouse with internal friction (RIF) model from general considerations of a discrete chain with local internal resistance, expressing its dynamics in terms of appropriate eigenfunctions and calculating the correct spatial dependence of the Langevin noise force. In the next section, we present the main new results of this paper, a calculation in closed-form of the end-to-end frequency response function of a RIF polymer, which in the limit of zero internal friction also gives the response of a Rouse chain. We then explore this response function in the regimes where internal and solvent friction dominate the slowest modes, and attempt to interpret the physics of our findings in terms of the real-space motion of the ends of the chain.

The RIF Model

To derive the Bazua and Williams,[13] and McInnes[17] form of local internal friction in polymer chains, we start with a model of discrete beads interconnected by springs of elastic constant κ, as in the Rouse model, but modify this picture to include an internal frictional force which opposes motion of the relative extension between two beads; i.e. $-\zeta_i(\dot{\boldsymbol{R}}_n - \dot{\boldsymbol{R}}_{n-1})$. This is equivalent to adding a dashpot of friction constant ζ_i in parallel to the spring between beads in the Rouse model, as shown in Figure 1. It is simple to see that the total force due to internal friction on the nth bead is the second-order difference in $\dot{\boldsymbol{R}}_n$: $\zeta_i(\dot{\boldsymbol{R}}_{n-1} - 2\dot{\boldsymbol{R}}_n + \dot{\boldsymbol{R}}_{n+1})$.

This is the force as derived from more microscopic considerations by Bazua and Williams[13] and was shown to be valid when the coarse-graining of the chain is on length scales larger than the persistence length of the chain. The Langevin equation of motion of the nth bead is then:

$$\zeta_s \frac{\mathrm{d}\boldsymbol{R}_n}{\mathrm{d}t} = \left(\kappa + \zeta_i \frac{\mathrm{d}}{\mathrm{d}t}\right)(\boldsymbol{R}_{n-1} - 2\boldsymbol{R}_n + \boldsymbol{R}_{n+1}) + \boldsymbol{f}_n \qquad (1)$$

where κ is the elastic constant between beads and $\boldsymbol{f}_n$ is the Langevin noise force. Within the Rouse framework, this equation phenomenologically describes a coarse-grained friction for any local conformational change; be it dihedral angle rotations that give rise to changes in bond orientation or, for example, chair-to-boat transitions in polysaccharides that effectively change the local bond length. To a good approximation, if N is large we can make a continuum approximation for the set of coupled differential equations represented by eq 1, to give the following PDE for the dynamics of a RIF polymer, represented as a space-curve $\boldsymbol{R}(n,t)$:

$$\zeta_s \frac{\partial \boldsymbol{R}}{\partial t} = \left(\kappa + \zeta_i \frac{\partial}{\partial t}\right)\frac{\partial^2 \boldsymbol{R}}{\partial n^2} + \boldsymbol{f}(n,t) \qquad (2)$$

We see that the RIF model introduces an extra term to the Rouse model, which is proportional to the rate of change of the coarse-grained curvature of the chain. Intuitively, the internal friction of a highly curved chain will depend on the dynamics of many local bond-hopping events on the chain, while the internal friction of a region with less curvature is dependent on relatively few local hops. This is the essence of the Kuhn theorem discussed by de Gennes[12] and is an idea that will be made more precise below in the normal-mode analysis of the dynamics of a RIF chain. Note that here, we do not attempt to include long-ranged hydrodynamic corrections due to Zimm,[2] since we are mainly interested in the response of the chain at high stretch ($Fb \gg k_BT$, where F is the tensile force applied to the polymer, b is Kuhn length and k_BT is Boltzmann's constant multiplied by heat-bath temperature), as commonly found in single molecule experiments. In this regime of stretching such corrections are only logarithmic in nature.

Mode Structure. The RIF equation has spatial eigenfunctions $\cos(p\pi n/N)$, for boundary conditions where the ends are free ($\partial_n\boldsymbol{R}|_{n=0} = \partial_n\boldsymbol{R}|_{n=N} = 0$) or $\sin([p - 1/2]\pi n/N)$, when one end is fixed and the other is free ($\boldsymbol{R}|_{n=0} = 0$; $\partial_n\boldsymbol{R}|_{n=N} = 0$). It is the latter set of boundary conditions that is most appropriate for analysis of AFM stretching experiments, when a constant force is maintained at one end. However, for simplicity we will present the calculations using the cosine basis, and simply note that there is a simple scaling, $\tau_R \rightarrow 4\tau_R$, for going from a cosine to sine basis, where τ_R is the Rouse time for the slowest mode of relaxation. The physical basis of this scaling lies in the doubling of wavelengths of each mode in the sine basis compared to the cosine, giving rise to a quadrupling of the relaxation times.

Using the Fourier series, $\boldsymbol{R}(n,t) = \boldsymbol{X}_0(t) + 2\sum_{p=1}^{\infty} \boldsymbol{X}_p(t) \cos(p\pi n/N)$, together with expressions for the Fourier coefficients, $\boldsymbol{X}_0(t) = 1/N \int_0^N \boldsymbol{R}(n,t)\, \mathrm{d}n$ and $\boldsymbol{X}_p(t) = 1/N \int_0^N \boldsymbol{R}(n,t) \cos(p\pi n/N)\, \mathrm{d}n$, the equation of motion of each mode is

$$\zeta_p \frac{\mathrm{d}\boldsymbol{X}_r(t)}{\mathrm{d}t} = -\kappa_p \boldsymbol{X}_p(t) + \boldsymbol{f}_p(t) \qquad (3)$$

Each mode is a spring and dashpot in parallel or dumbbell, with elastic constant κ_p, friction constant ζ_p and relaxation time τ_p; the elastic constants of each mode are unchanged from the standard Rouse description

$$\kappa_p = \frac{2\pi^2 p^2 \kappa}{N} \quad \text{for } p \geq 0 \qquad (4)$$

but the mode friction is renormalized to

$$\zeta_0 = N\zeta_s;\ \zeta_p = 2N\zeta_s + \frac{2\pi^2 p^2 \zeta_i}{N} \quad \text{for } p > 0 \qquad (5)$$

So we see, as many previous authors have found, internal friction has the character of scaling inversely with the number of monomers N. As expected internal friction does not play a role in the motion of the center of mass. The mode relaxation

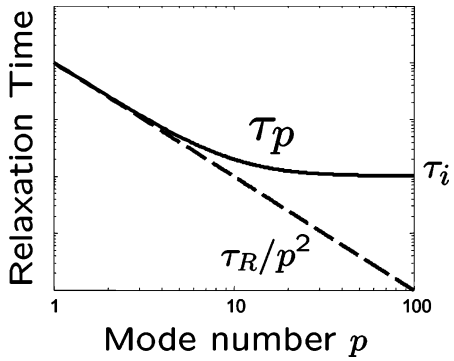

Figure 2. Log−log plot of relaxation time of modes in RIF model plotted as a function of mode number p, compared with those of the standard Rouse model ($\tau_R > \tau_i$).

times ($\tau_p = \zeta_p/\kappa_p$) in the RIF model are also renormalized:

$$\tau_p = \frac{\zeta_p}{\kappa_p} = \frac{\tau_R}{p^2} + \tau_i \tag{6}$$

where

$$\tau_R = \frac{N^2\zeta_s}{\pi^2\kappa} \tag{7}$$

is the Rouse time for a polymer with free ends and

$$\tau_i = \frac{\zeta_i}{\kappa} \tag{8}$$

is the relaxation time of the polymer due to internal friction processes.

We see that relaxation due to internal friction happens with a fixed time, independent of mode number, since both the mode internal friction and elasticity have the same, p^2, dependence on curvature.[24] Plotted in Figure 2 is the mode relaxation time τ_p vs mode number p, for the case where $\tau_R > \tau_i$, showing that when $\tau_R/p^2 \sim \tau_i$, there is a transition from solvent friction dominated relaxation to one where internal friction dominates. If we consider only the relaxation of the first mode ($p = 1$), then this relation indicates that solvent friction will dominate for chains longer than

$$N \gg \pi\sqrt{\zeta_i/\zeta_s} \tag{9}$$

which is a specific restatement of Kuhn's theorem[12,16] within the framework of the RIF model. However, as eq 5 shows the internal friction of shorter wavelength modes increases as p^2, hence, the comparison, $\tau_R/p^2 \sim \tau_i$, also gives a critical mode number, above which internal friction dominates relaxation:

$$p_c \sim \sqrt{\frac{\tau_R}{\tau_i}} = \frac{N}{\pi}\sqrt{\frac{\zeta_s}{\zeta_i}} \tag{10}$$

Modes with a mode number larger than p_c, will be dominated by internal friction for all frequencies. This will be seen more explicitly later, when we calculate the frequency response function of the ends of the chain.

It is eq 10 that justifies the general neglect of internal friction in modeling the dynamics of long polymer chains in melts and dilute solutions. However, as shown previously,[10] internal friction has a strong dependence on chain tension, F, which modifies this picture considerably at high stretch ($Fb \gg k_BT$). On one hand tension at high stretch will deform local barriers to conformational change, which in turn will alter the chain internal friction in a non-trivial manner. However, in addition, as predicted by the *frictional* freely jointed chain (FFJC) model,[10] chain internal friction can increase monotonically with tension at high stretch in a very general way. In contrast, solvent friction has a relatively weak dependence on chain tension at high stretch, so that it is possible for chain internal friction to dominate for *any* chain length, if subject to a sufficiently large tension, such as in single molecule experiments.[4−10]

Spatial Noise Correlation. In the Rouse model, the Langevin noise force is assumed to act independently on each bead and to be uncorrelated in time so that $\langle \boldsymbol{f}(n,t)\boldsymbol{f}^{\dagger}(m,t')\rangle = 2k_BT\zeta_s\boldsymbol{I}\delta(n-m)\delta(t-t')$, where $\boldsymbol{I}$ is the 3×3 unit identity matrix. However, in the RIF model, it is clear that with the introduction of an internal friction force that acts *between* beads, the assumption of spatially white Langevin noise is no longer valid. In this section, we calculate the spatial dependence of the noise for monomers n and m.

Although, we have not explicitly expressed the moments of the Langevin force, the correlations of the noise for the modes can be deduced to have the following property:

$$\langle \boldsymbol{f}_p(t)\rangle = 0;\ \langle \boldsymbol{f}_p(t)\boldsymbol{f}_q^{\dagger}(t')\rangle = 2k_BT\zeta_p\boldsymbol{I}\delta_{pq}\delta(t-t') \tag{11}$$

as required to ensure that the chain end-to-end vector obeys equipartition ($\langle R^2\rangle = 16\sum_p\langle \boldsymbol{X}_p^{\dagger}\boldsymbol{X}_q\rangle = 3k_BT/\kappa_R = 3k_BT/(\kappa/N)$). From this we can calculate the real-space noise correlations. Using the Fourier series decomposition of $\boldsymbol{f}(n,t) = 1/N(\boldsymbol{f}_0(t) + \sum_{p=1}^{\infty}\boldsymbol{f}_p(t)\cos(p\pi n/N))$, we can calculate the second moment of this noise using eq 11 and eq 5:

$$\langle \boldsymbol{f}(n,t)\boldsymbol{f}^{\dagger}(m,t')\rangle = 2k_BT\delta(t-t')\boldsymbol{I}\left(\zeta_s\delta(n-m) + \frac{2\pi^2\zeta_i}{N^3}\sum_{p=1}^{\infty}p^2\cos\left(\frac{p\pi n}{N}\right)\cos\left(\frac{p\pi m}{N}\right)\right) \tag{12}$$

However, the p^2 factor in the summation will cause the internal friction force variance to diverge, which is a simple consequence of the continuum limit of an ultimately discrete problem. Fortunately, as we shall see in the next section, since the nature of internal friction is to act mechanically in series, these high spatial frequency anomalies of the continuum description do not affect the large scale properties of the chain like the internal friction of the end-to-end vector. We can, however, simplify the above expression further if we terminate the sum at $p = N$, the smallest wavelength of a discrete chain, and approximate the sum as an integral in the large N limit. This gives

$$\langle \boldsymbol{f}(n,t)\boldsymbol{f}^{\dagger}(m,t')\rangle = 2k_BT\delta(t-t')\boldsymbol{I}\left(\zeta_s\delta(n-m) + 2\zeta_i\frac{(-1)^{n-m}}{(n-m)^2}\right) \tag{13}$$

where we have used the fact that if $n - m$ is odd (even), then so is $n + m$, for integer n, m and that to a very good approximation the fast varying term $\sim(n+m)^{-2}$ can be considered negligible. This result indicates, as expected, that the internal friction part of this fluctuation−dissipation relation is spatially *colored*. In addition, the force on a pair of beads is anticorrelated for odd separation, $n - m$, but positively

correlated for even separation. This follows from the fact that adjacent beads must have an equal and opposite force on each other.

End-to-End Response and Correlations of the RIF Model

In this section, we will see how the relationship between solvent and internal friction and their respective relaxation times is expressed through the response and correlation functions of the end-to-end vector of a RIF polymer. The main result of this section and this paper, are closed form expressions of the frequency response function of both the Rouse and RIF models. The approach we will take is to calculate the frequency response, or dynamic compliance, of the end-to-end vector, by summing over all odd modes using the properties of the Digamma function (see Appendix). From the closed form expression of the end-to-end response, the fluctuation−dissipation theorem can be used to calculate the power spectrum of fluctuations of the RIF model, which is of particular importance when comparing to experiments that measure the fluctuations of single biopolymers.

Dynamic Compliance of RIF Polymer. The end-to-end vector of the chain is given by

$$\boldsymbol{R}(t) = \boldsymbol{R}(N, t) - \boldsymbol{R}(0, t) = -4 \sum_{p:\text{odd}}^{\infty} \boldsymbol{X}_p(t) \tag{14}$$

Only odd p modes contribute to the end-to-end vector, since these are the only modes that have a net displacement over the length of the polymer backbone, from $n = 0$ to $n = N$. Modes are uncorrelated such that the cross-correlation of mode amplitudes is $\langle \boldsymbol{X}_p(0)\boldsymbol{X}_q^{\dagger}(t)\rangle = \delta_{pq}\alpha_p(t)\boldsymbol{I}$, where $\alpha_p(t) = k_BT/\kappa_p e^{-t/\tau_p}$ is the autocorrelation function of the pth dumbbell mode. Using the relation eq 14, it is then straightforward to express the autocorrelation of the fluctuations of the end-to-end vector as

$$\alpha_{\boldsymbol{R}}(t) = \langle \boldsymbol{R}(0)\boldsymbol{R}^{\dagger}(t)\rangle = 16\boldsymbol{I} \sum_{p:\text{odd}}^{\infty} \frac{k_BT}{\kappa_p} e^{-t/\tau_p} \tag{15}$$

The fluctuation dissipation theorem (FDT) is a fundamental relationship between the equilibrium random fluctuations of a system subject to Brownian motion and its linear Green's response. Here, we use its time-domain form,[3] $\mathcal{J}(t) = -1/k_BT\ \mathrm{d}/\mathrm{d}t\ \alpha(t)$, to calculate the Green's response of R:

$$\mathcal{J}_R(t) = 16 \sum_{p:\text{odd}}^{\infty} \frac{1}{\zeta_p} e^{-t/\tau_p} \tag{16}$$

where we are now only considering fluctuations in a single direction, say, the stretching direction in a single molecule experiment. Taking the Fourier transform of this gives the dynamic compliance or frequency response as

$$J_R(\omega) = 16 \sum_{p:\text{odd}}^{\infty} \frac{1}{\kappa_p} \frac{1}{1 + i\omega\tau_p} \tag{17}$$

We will now evaluate this summation for the RIF model; the response function of a standard Rouse chain can then be found by setting $\zeta_i = 0$, which as can be seen when examining eq 2, will recover standard Rouse dynamics. To proceed, we can rearrange the summation in eq 17 using eq 6, in terms of an index k that runs over all positive integers:

$$J_R(\omega) = \frac{8N}{\pi^2\kappa} \frac{1}{(1 + i\omega\tau_i)} \sum_{k=1}^{\infty} \frac{1}{(2k-1)^2 + \dfrac{i\omega\tau_R}{1 + i\omega\tau_i}} \tag{18}$$

In the Appendix, we show, using the properties of the Digamma function $\Psi(z) = \mathrm{d}/\mathrm{d}z\ \ln\Gamma(z)$, that the sum above is given by the following useful expression,

$$\sum_{k=1}^{\infty} \frac{1}{(2k-1)^2 - z^2} = \frac{\pi}{4z} \tan\left(\frac{\pi z}{2}\right) \tag{19}$$

Hence, making the identification $-z^2 = \sqrt{i\omega\tau_R/(1+i\omega\tau_i)}$, we find a closed-from expression for the RIF end-to-end frequency response:

$$J_R(\omega) = \frac{2N}{\pi\kappa} \frac{\tanh\left(\dfrac{\pi}{2}\sqrt{\dfrac{i\omega\tau_R}{1 + i\omega\tau_i}}\right)}{\sqrt{i\omega\tau_R(1 + i\omega\tau_i)}} \tag{20}$$

From this expression, it is then simple to calculate the power spectral density (PSD), $P_R(\omega)$, from the imaginary part of the response function $J_R''(\omega)$, using the frequency-domain version of the FDT, $P_R(\omega) = -2k_BT/\omega\ J_R''(\omega)$.[20,21]

To examine the behavior of a Rouse chain with and without internal friction, we plot the real and imaginary parts of the RIF response function (eq 20) in Figure 3, for different ratios of internal to solvent friction, where the case $\tau_i/\tau_R = 0$ corresponds to the Rouse response (eq 21). In the limit of large internal friction, $\zeta_i \gg \zeta_s$,[25] the response is single-mode or dumbbell-like with the real and imaginary parts decaying as ω^{-2} and ω^{-1}, respectively; at high frequencies ($\omega\tau_i \gg 1$), the response of the dumbbell is dominated by dissipation. In contrast, we see that the Rouse response is characterized by a $\omega^{-1/2}$ scaling behavior at high frequency ($\omega\tau_R \gg 1$), for both the real and imaginary parts; the response is equally elastic and dissipative at high frequencies, indicating that the continuum Rouse chain has structure and thus modes relaxing on all length scales. This is unrealistic as it stands, as physically we expect a lower length scale cutoff for relaxation of the backbone, which is of the order the monomer size. However, we see that this is somewhat remedied in the RIF model, when internal friction is finite. If the internal friction constant is nonzero, but the slowest mode is dominated by solvent friction ($\tau_R \gg \tau_i$), we see Rouse-like behavior at low frequency, which persists up to a critical frequency τ_i^{-1}, corresponding to the relaxation of modes satisfying the relation, $\tau_R/p^2 \sim \tau_i$. At greater frequencies the real and imaginary parts of the response function decay with dumbbell-like scaling behavior, indicating that dissipation dominates the elastic response due to the large internal friction of high curvature modes. Qualitatively, the introduction of local internal friction in the continuum Rouse chain, thus provides a phenomenological means of reintroducing a certain type of discreteness, through a lower time scale, τ_i, and length scale, $\lambda \sim b\pi\sqrt{\zeta_i/\zeta_s}$ (i.e., the wavelength of the critical model number in eq 10) for relaxation; modes smaller than this wavelength are, in effect, dynamically frozen due to their large internal friction.

In the next sections we take appropriate limits of eq 20, to quantify the regimes where Rouse and dumbbell like behavior dominate for a RIF polymer, discussing the underlying physics of the chain in these limits.

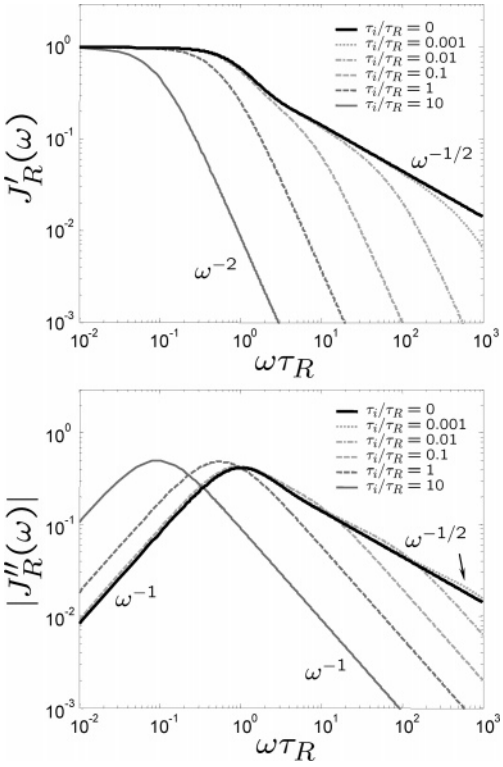

Figure 3. Real (top) and imaginary (bottom) part of RIF frequency response, for different ratios of internal friction to solvent friction, indicated by their respective relaxation times τ_i and τ_R.

Rouse Model, $\tau_i = 0$. To calculate the response function of the ends of a Rouse chain, we simply set $\zeta_i = 0$ in eq 20:

$$J_R(\omega) = \frac{2N}{\pi\kappa}\frac{\tanh\left(\frac{\pi}{2}\sqrt{i\omega\tau_R}\right)}{\sqrt{i\omega\tau_R}} \tag{21}$$

In the limit, $\omega\tau_R \to 0$, $J_R(\omega \to 0) = N/\kappa = 1/\kappa_R$; as we expect the response is purely elastic with a constant κ_R, the static stretching elastic constant of the chain. At high frequency ($\omega\tau_R \gg 1$), the tanh function returns unity, and it is simple to see that the response is given by, $J_R \sim 1/\sqrt{i\omega\tau_R}$, which is equal in its real and imaginary parts, as observed from Figure 3. To understand why the Rouse chain response decays as $(\omega\tau_R)^{-1/2}$, we observe that the Rouse equation (eq 2 with $\zeta_i = 0$) is a one-dimensional diffusion equation for perturbations along the backbone, with diffusion constant, $D_n \sim \kappa/\zeta$. The distance a perturbation travels in a time t is thus governed by the usual diffusion law, $n^2 \sim D_n t$, and so an oscillation of the end of the chain at frequency ω, can only penetrate a distance,[26]

$$n^*_R(\omega) \sim \sqrt{D_n/\omega} \tag{22}$$

The effective compliance of the chain is then $J_R(\omega) \sim (\kappa/n^*_R(\omega))^{-1} \sim 1/\sqrt{\kappa\zeta\omega}$, which agrees with the high-frequency limit of eq 21. Interestingly, we note that at high frequency, the dynamic compliance is independent of chain length N, since we are only probing the local structure of the chain.

RIF Model: Internal Friction Always Dominates, $\tau_i \gg \tau_R$. This regime is characterized by *short* chains as defined by eq 9. Equation 20 can be rearranged to give

$$J_R(\omega) = \frac{2N}{\pi\kappa}\frac{\tanh\left(\frac{\pi}{2}\sqrt{\frac{\tau_R/\tau_i}{\frac{1}{i\omega\tau_i}+1}}\right)}{\sqrt{i\omega\tau_R(1+i\omega\tau_i)}} \tag{23}$$

If we let z be the argument of the tanh function then as $\omega\tau_i \to \infty$, the argument $z \to \pi/2\sqrt{\tau_R/\tau_i}$. In addition, when $\omega\tau_i \to 0$, $z \to 0$ and so together $z \ll 1\ \forall\ \omega$. For small z, $\tanh z \approx z$ and it is then simple to show that the dynamic compliance of the RIF model, when $\tau_i \gg \tau_R$ is

$$J_R(\omega) = \frac{N}{\kappa}\frac{1}{1+i\omega\tau_i} \tag{24}$$

which is the response of a simple dumbbell with friction ζ_i/N and elastic constant κ/N. This shows that a polymer with many beads and degrees of freedom, but dominated by internal friction, acts like a dumbbell with a single degree of freedom, where the relaxation of faster or small-wavelength modes are effectively frozen out due to their slowness in changing conformation. However, as for the analysis of the Rouse chain, we can examine the dynamics of the chain in real space. When internal friction is dominant each part of the chain responds with the same average time τ_i, and so a perturbation applied to the end of a dumbbell propagates exponentially, as $n(t) = N(1 - e^{-t/\tau_i})$ on average. If we now consider the chain end being oscillated at a frequency ω, we see only a fraction of the chain length, $n^*_D(\omega) = N(1 - e^{-1/\omega\tau_i})$, can respond; if $\omega\tau_i \ll 1$, the perturbation propagates the whole chain ($n^*_D(\omega) \to N$), while if $\omega\tau_i \gg 1$, a Taylor expansion shows,

$$n^*_D(\omega) \sim \frac{N}{\omega\tau_i} \tag{25}$$

This result gives the high-frequency response to be $|J(\omega)| = n^*_D(\omega)/\kappa \sim N/\omega\zeta_i$, which agrees with the high-frequency limit of eq 24 above. In summary, at high-frequency perturbations influence only a finite length of a dumbbell in a frequency dependent manner, as for the Rouse chain, leading to a decreasing compliance at high-frequency. However, unlike the Rouse chain, this length is not a penetration length, but represents the fraction of the chain that can respond on a time scale ω^{-1} and so depends on the total chain length N.

RIF Model: Solvent Friction Dominates Slowest Mode, $\tau_R \gg \tau_i$. This regime would be characterized by *long* chains as defined by eq 9. Here there are two regimes, as indicated in Figure 3, demarcated by the characteristic relaxation time of internal friction. When $\omega\tau_i \ll 1$, it is simple to see that the RIF response will be Rouse-like as given by eq 21. However, at high frequency $\omega\tau_i \gg 1$, the dynamic compliance becomes

$$J_R(\omega) \approx \frac{2N}{\pi\kappa}\frac{1}{i\omega\sqrt{\tau_R\tau_i}} = \frac{2}{i\omega\sqrt{\zeta_s\zeta_i}} \tag{26}$$

where we have used $\tanh(z \to \infty) \to 1$. This is effectively the high-frequency friction-dominated behavior of a dumbbell, as observed in Figure 3 for $\tau_i/\tau_R \le 0.1$, but with a relaxation time which is the geometric average of the solvent and internal friction relaxation times, $\sqrt{\tau_R\tau_i}$. Equivalently, we can consider the effective friction in this regime to be $\sqrt{\zeta_s\zeta_i}$. However, unlike the internal friction dominated high-frequency response, which depends on the length of chain, the high-frequency response of a Rouse chain with finite friction does not depend

on N. A real-space analysis, again provides some illumination. As for the Rouse chain, perturbations will propagate diffusively on the time scale τ_R, but in addition for a RIF chain, perturbations also propagate in an exponential manner due to the presence of internal friction. In the regime we are considering $\tau_R \gg \tau_i$, so that as long as $\omega\tau_i \ll 1$ the penetration length will be as for the Rouse chain: $n^*_{RIF}(\omega) = \sqrt{D_n/\omega}$. At, and beyond the critical frequency $\omega = 1/\tau_i$, exponential dumbbell relaxation becomes important due to internal friction, so that when $\omega\tau_i \gg 1$, $n^*_{RIF}(\omega)$ is dumbbell-like, but with a maximum accessible chain length limited by diffusion, which from eq 22 is given by $n_R(\omega = \tau_i^{-1}) = \sqrt{D_n\tau_i}$. Using eq 25, the length of chain that responds is given by

$$n^*_{RIF}(\omega) = \frac{n_R(\omega = \tau_i^{-1})}{\omega\tau_i} = \frac{\kappa}{\omega\sqrt{\zeta_s\zeta_i}} \tag{27}$$

Calculating the response $|J(\omega)| = n^*_{RIF}/\kappa$ then agrees with the high-frequency limit of the more formal calculation in eq 26. We see that although at high-frequency the RIF response is dumbbell-like, it is independent of chain length, since for long enough chains, Rouse diffusion is always slow enough to ensure that only a finite length of the chain can be probed. Conversely, as we have seen, in the regime where internal friction always dominates (i.e., *short* chains), Rouse diffusion is relatively fast so that the whole chain is probed and the response is dependent on N.

Applications to Experiments

There has been much recent interest in stretching experiments that measure the viscoelasticity of single biomolecules with a view to measuring local dynamical properties not possible using conventional force spectroscopy.[4−10] These experiments have employed either a direct oscillation of an AFM tip, observing the change in amplitude and phase with frequency or more simply calculate the power spectrum density of the thermal fluctuations of the tip. As long as the amplitude of oscillations are sufficiently small, the fluctuation−dissipation theorem guarantees that both approaches are in principle equivalent. Taking the latter approach, the thermal fluctuations of two polysaccharides, cellulose and dextran, were modeled using the RIF model response eq 20, determining the effective elastic, solvent and internal friction constants of the single molecules.[10] The results indicated that, in the high stretch regime, internal friction dominated dissipation for these biopolymers and hence, the molecular weight of the polymers measured ($N \approx 400$) are in the regime of being classified "short" in accord with the definition of eq 9. The importance of the RIF model in this work, was in its ability to unequivocally identify the friction measured in these stretching experiments, with internal conformational friction of the polymer. So experiments to date are consistent with predictions of the RIF model in the regime where internal friction is dominant, but have not provided a test for the its more interesting predictions, for example, in the regime where solvent friction dominates the slowest dynamic modes.

The simplest way to test these predictions would be to use longer polymers; assuming a similar degree of stretch, such that the monomeric internal friction constant $\zeta_i \sim 10 \rightarrow 100$ μg kHz,[4−10] and a monomer solvent friction constant of $\zeta_s \sim 10^{-5}$ μg kHz ($\zeta_s = 6\pi\eta b$, where $b \sim 1$ nm), together with eq 9, would suggest that polymers of length, $N \gg 1000$, will be dominated by solvent friction in the slowest modes. However, higher molecular weight polymers have a problem with detectability in AFM single molecule experiments; the larger compliance of long molecules requires very soft tips, in addition to an overall pick-up probability that, empirically, is found to be small. Chemically specific attachment strategies or alternative experimental methods such as magnetic or optical tweezers may overcome these issues. Using AFM it is also difficult to measure the response, or PSD, of a single molecule directly, since the small dynamic compliance of the cantilever tip tends to mask the larger dynamic compliance of the single molecule, due to the mechanically parallel combination of molecule and cantilever.[10] Again softer and smaller AFM tips or the use of optical or magnetic tweezers, which would all have reduced elastic and friction constants should allow a more direct measurement of single-molecule fluctuations or responses.

A further consequence for single molecule stretching experiments is the frequency-dependent length of chain that can respond to perturbations, which resulted from the real-space analysis of the response of a RIF chain. When solvent friction dominates the slowest modes it was found that this length (eq 27) is independent of chain length,[27] which suggests that the results of probing polymers that are "long" according to the definition in eq 9, would be due only to monomers closest to the probe. This has implications for applying such techniques to examine the structure of heterogeneous polymers such as proteins. Conversely, when internal friction dominates all modes of the chain, as is the case in previous single molecule viscoelasticity experiments,[4−10] the length of chain that can respond (eq 25) is dependent on chain length and the whole chain is probed.

Summary and Conclusions

In this paper, we have investigated the dynamical properties of a Rouse polymer model that includes a coarse-grained source of local internal friction. First, we calculated the mode-structure in terms of appropriate eigenfunctions and then the correct spatial dependence of the Langevin noise variance of a Rouse chain with internal friction (RIF). Summing over the response functions of each mode that contributes to the end-to-end vector and using the properties of the Digamma function, resulted in a closed-form expression for the frequency response function of a RIF polymer. This result showed that the clear signatures of the dominance of internal friction and solvent friction are a dumbbell and Rouse-like frequency response, which are characterized at high frequency by $|J(\omega)| \sim \omega^{-1}$ and $|J(\omega)| \sim \omega^{-1/2}$, respectively. In addition, we found a quantitative realization of Kuhn's theorem; if solvent friction dominates the slowest, long wavelength mode, then there will be a critical mode number, whose curvature and thus internal friction is large enough to cause a switch from Rouse-like to a dumbbell-like response. A more intuitive real-space analysis revealed that in the case of the Rouse model, propagation occurs diffusively giving rise to a penetration length from the end of the chain that is independent of chain length, while for a dumbbell, propagation occurs in an exponential manner that does depend on chain length. In the case of a RIF chain, if solvent friction dominates the slowest modes, exponential dumbbell-like propagation occurs with a maximum accessible chain length that is limited by diffusion. The last finding implies that the results of single molecule stretching experiments that probe heterogeneous polymers need to be carefully interpreted. In summary, the generic coarse-grained model presented provides a means of correctly quantifying dissipation due to solvent and that due to internal conformational changes within flexible biopolymers. As shown elsewhere,[10] it is the latter component of dissipation that contains

new information on the local dynamics of biomolecules on an underlying energy landscape of conformational change.

Acknowledgment. We thank Armand Ajdari, Physico-Chimie Théorique, Ecole Supérieure de Physique et de Chimie Industrielles, Paris and Peter Olmsted, School of Physics and Astronomy, University of Leeds, for insightful comments on this work during the PhD viva of B.S.K. We also thank Masaru Kawakami, School of Materials Science, Japan Advanced Institute of Science and Technology for discussions on experimental issues. We thank the Engineering and Physical Sciences Research Council (EPSRC) UK, for financial support. T.C.B.M. was an EPSRC Senior Fellow.

Appendix: The Digamma Function and Summation Over Rouse Modes

The Digamma function is defined to be the derivative of the natural logarithm of the Gamma function,

$$\Psi(z) = \frac{\mathrm{d}}{\mathrm{d}z} \ln(\Gamma(z)) \tag{28}$$

In this appendix we show how to use a series expansion of $\Psi(z)$, to calculate the effective end-to-end response of Rouse-like chains. One definition of the Gamma function is due to Euler:

$$\Gamma(z) = \lim_{k\to\infty} \left\{ \frac{k!k^z}{z(z+1)(z+2)\ldots(z+k)} \right\} \tag{29}$$

Using the identity $\Gamma(1+z) = z\Gamma(z)$ and eq 28, $\Psi(1+z)$ can be expressed as follows:

$$\Psi(1+z) = -\gamma + \sum_{k=1}^{\infty} \frac{z}{k(z+k)} \tag{30}$$

where γ is the Euler−Mascheroni constant. From eq 18, the frequency response function of the end-to-end vector is given by

$$J_R(\omega) \sim \sum_{k=1}^{\infty} \frac{1}{(2k-1)^2 + \dfrac{i\omega\tau_R}{1+i\omega\tau_i}} \sim \sum_{k=1}^{\infty} \frac{1}{k^2 - k + \dfrac{1}{4} + \dfrac{1}{4}\dfrac{i\omega\tau_R}{i\omega\tau_i}} \tag{31}$$

As a first guess, using eq 30, we form the sum $\Psi(z) - \Psi(-z)$ to obtain

$$\Psi(z) - \Psi(-z) = \sum_{k=1}^{\infty} \frac{2z}{k^2 - 2k + 1 - z^2} \tag{32}$$

which is close but not quite what is required. To calculate eq 31, we use a more general approach:

$$\Psi(f(z)) - \Psi(f(-z)) = \sum_{k=1}^{\infty} \left(\frac{f(z)-1}{n(n+f(z)-1)} - \frac{f(-z)-1}{n(n+f(-z)-1)} \right) = \sum_{k=1}^{\infty} \frac{f_z - f_{-z}}{k^2 + k(f_z + f_{-z} - z) + f_z f_{-z} - (f_z + f_{-z}) + 1} \tag{33}$$

Equating the relevant coefficients with eq 31, we find

$$f_z + f_{-z} = 1 \tag{34}$$

$$f_z f_{-z} = g(z) + \frac{1}{4} \tag{35}$$

where $g(z)$ has no constant terms and will be equated to $^1/_4 i\omega\tau_R/(1+i\omega\tau_i)$. The function $f(z) = {}^1/_2(1+z)$ satisfies both these equations and hence

$$\Psi\left(\frac{1}{2}(1+z)\right) - \Psi\left(\frac{1}{2}(1-z)\right) = \sum_{k=1}^{\infty} \frac{z}{k^2 - k + \dfrac{1}{4} - z^2/4} \tag{36}$$

To simplify this further, we use the standard identity[23] $\Psi(z) = \Psi(1-z) - \pi\cot\pi z$ to show that

$$\Psi\left(\frac{1}{2}(1+z)\right) - \Psi\left(\frac{1}{2}(1-z)\right) = \pi\tan\left(\frac{\pi z}{2}\right) \tag{37}$$

So finally we arrive at the main mathematical result eq 19, which is used to evaluate the sum given in eq 31:

$$\sum_{k=1}^{\infty} \frac{1}{(2k-1)^2 - z^2} = \frac{\pi}{4z}\tan\left(\frac{\pi z}{2}\right) \tag{38}$$

References and Notes

(1) Rouse, P. *J. Chem. Phys.* **1953**, *21*, 1272−1280.
(2) Zimm, B. *J. Chem. Phys.* **1956**, *24*, 269.
(3) Doi, M.; Edwards, S. *The Theory of Polymer Dynamics;* Oxford University Press: Oxford, U.K., 1986.
(4) Humphris, A.; Tamayo, J.; Miles, M. *Langmuir* **2000**, *16*, 7891−7894.
(5) Humphris, A.; Antognozzi, M.; McMaster, T.; Miles, M. *Langmuir* **2002**, *18*, 1729−1733.
(6) Janovjak, H.; Müller, D. J.; Humphris, A. D. L. *Biophys. J.* **2005**, *88*, 1423−1431.
(7) Kawakami, M.; Byrne, K.; Khatri, B.; Mcleish, T. C. B.; Radford, S. E.; Smith, D. A. *Langmuir* **2004**, *401*, 400−403.
(8) Kawakami, M.; Byrne, K.; Khatri, B.; Mcleish, T. C. B.; Radford, S. E.; Smith, D. A. *Langmuir* **2005**, *21*, 4765−4772.
(9) Kawakami, M.; Byrne, K.; Brockwell, D. J.; Radford, S. E.; Smith, D. A. *Biophys. J.* **2006**, *91*, L16−L18.
(10) Khatri, B. S.; Kawakami, M.; Byrne, K.; Smith, D. A.; McLeish, T. C. B. *Biophys. J.* **2007**, *92*, 1825−1835.
(11) Poirier, M. G.; Marko, J. F. *Phys. Rev. Lett.* **2002**, *88*, 228103.
(12) de Gennes, P. G. *Scaling Concepts in Polymer Physics;* Cornell University Press: Ithaca, NY, 1985.
(13) Bazua, E. R.; Williams, M. C. *J. Chem. Phys.* **1973**, *59*, 2858−2868.
(14) Guyon, E.; Hulin, J.; L.Petit,; Mitescu, C. *Physical Hydrodynamics;* Oxford University Press: Oxford, U.K., 2001.
(15) Manke, C. W.; Williams, M. C. *Macromolecules* **1985**, *18*, 2045−2051.
(16) Kuhn, W.; Kuhn, H. *Helv. Chim. Acta* **1945**, *28*, 1533.
(17) Pugh, D.; MacInnes, D. A. *Chem. Phys. Lett.* **1975**, *34*, 139−142.
(18) McInnes, D.; North, A. *Polymer* **1977**, *18*, 505−508.
(19) MacInnes, D. A. *J. Polym. Sci.* **1977**, *15*, 657−674.
(20) de Groot, S.; Mazur, P. *Non-equilibrium Thermodynamics;* Dover Publications: New York, 1984.
(21) Landau, L.; Lifshitz, E. *Statistical Physics;* Pergamon Press: Oxford, U.K., 1980.
(22) Landau, L.; Lifshitz, E. *Fluid Mechanics*, 2nd ed.; Pergamon Press: Oxford, U.K., 1987.
(23) Abramowitz, M.; Stegun, I. A. E. *Handbook of Mathematical Functions with Formulas, Graphs, and Mathematical Tables*, 9th ed.; Dover: New York, 1972; Chapter 6 (§6.3), pp 258−259.
(24) The fact that the relaxation time of the modes is independent of mode number is not in contradiction with the concept of the internal friction and hence dynamic flexibility of a mode decreasing with curvature. As was shown in ref 10, the microscopic internal friction constant is

controlled by an average *hopping time*, which is in general distinct to the relaxation time.

(25) The relationship, $\zeta_i \gg \zeta_s$, is not equivalent to the relationship, $\tau_i \gg \tau_R$, since there is a factor π^2, which multiplies the ratio ζ_{sR}/κ_R in the definition of τ_R. So for example, when $\tau_i/\tau_R = 1$, $\zeta_i/\zeta_s = \pi^2 \sim 10$ and internal friction dominates the response.

(26) The physics described is analogous to high-frequency models of Brownian motion[22] or the skin-effect in conductors, where an oscillating influence can only penetrate a certain distance, due to the finite time of diffusion.

(27) This is also true for a Rouse chain (eq 22), however, in this idealized case the internal friction is zero and the internal properties of the chain cannot be probed.

MA071175X